

Local Statistics for Spatial Panel Models with Application to the US Electorate

Jianfeng Wang, Adam B Kashlak
Mathematical & Statistical Sciences
University of Alberta
Edmonton, Canada, T6G 2G1

October 22, 2021

Abstract

The spatial panel regression model has shown great success in modelling econometric and other types of data that are observed both spatially and temporally with associated predictor variables. However, model checking via testing for spatial correlations in spatial-temporal residuals is still lacking. We propose a general methodology for fast permutation testing of local and global indicators of spatial association. This methodology extends past statistics for univariate spatial data that can be written as a gamma index for matrix similarity to the multivariate and panel data settings. This includes Moran's I and Geary's C among others. Spatial panel models are fit and our methodology is tested on county-wise electoral results for the five US presidential elections from 2000 to 2016 inclusive. County-wise exogenous predictor variables included in this analysis are voter population density, median income, and percentage of the population that is non-hispanic white.

1 Introduction

Few datasets are more intriguing than those surrounding national elections. Trying to determine which factors influence the whims of the electorate is of importance for both historical study and future predictions. Political and demographic data naturally exists in a spatial temporal setting. One tool for modelling such data is the spatial panel regression model, which combines panel data analysis—i.e. where measurements are taken on the same units over an extended time period—with a spatial dependency network. Details and references are in Section 1.1.

Beyond mere modelling of political performance using spatial panel models, we are interested in the model's performance in fitting to the data. To this end, we extend a variety of local indicators of spatial association (LISA) to apply to the residuals produced by spatial panel models. Furthermore, these test statistics are evaluated via a quick to compute analytic variant of the classic permutation test with details and references in Section 1.2. This allows for fast exact testing of regression residuals for local spatial association across a large graphical network. We will test our methods on a data set of 5 years \times 3104 counties worth of electoral and demographic data.

The US elections and demographics data is introduced in Section 2. Some regressions and plots are displayed to give a picture of the data under consideration. A variety of multivariate LISA statistics are introduced in Section 3.1 and non-asymptotic exact significance testing of such statistics is discussed in Section 3.2. A simulation study on a 50×60 rectangular grid is performed in Section 4 to compare four LISA statistics on multivariate Gaussian data. Fitted

spatial panel models on the US elections data are detailed in Section 5.1. LISA tests for the US data are performed in Section 5.2, and a comparison of the performance of these methods on this real world data is detailed in Section 5.3.

1.1 Spatial Panel Models

The spatial panel data regression model (Anselin et al., 2001; Baltagi et al., 2003; Kapoor et al., 2007; Baltagi, 2008) extends panel data models into the spatial realm by accounting for both random region effects and spatially autocorrelated residuals. This model can be fit to data via the `splm` R package (Millo and Piras, 2012).

For y_t being the observation vector from all regions at time t , we have

$$y_t = \lambda W y_t + X_t \beta + u_t \quad (1.1)$$

$$u_t = \rho W u_t + \varepsilon_t \quad (1.2)$$

$$\varepsilon_t = \mu + v_t \quad (1.3)$$

from Kapoor et al. (2007). The model in Baltagi et al. (2003) is nearly identical but with a few swapped terms. Equation 1.1 models the observations based on the $n \times p$ matrix of non-stochastic predictors X_t at time t and unknown regression coefficients β . Additionally, y can have a spatial lag determined by estimating $|\lambda| < 1$ and the user selected weight matrix W . The u_t in Equation 1.2 is a spatially autocorrelated process depending on parameter $|\rho| < 1$. Equation 1.3 models the innovations vector as μ , a regional random effect with variance σ_μ^2 , and v_t , iid mean zero normal errors with variance σ_v^2 . Within the `splm` package, the function `spgm` fits the above model using the generalized moments estimator from Kapoor et al. (2007) In contrast, the function `spml` fits a similar model using maximum likelihood as outlined in Baltagi et al. (2003). Details on both methods can be found in Millo and Piras (2012). In this article, we will fit the model defined by 1.1, 1.2, and 1.3 using `spgm`.

1.2 Permutation Testing

There are two paradigmatic approaches to statistical hypothesis testing for spatial data models: asymptotic normality and permutation testing. The former method is popular due to the rapidity of producing a p-value, but relies on strong data assumptions and a large enough sample size to be “asymptotic”. Much past research (Anselin, 1995, 2019; Seya, 2020) suggests use of a permutation test instead of the normal approximation. The permutation test (Mielke and Berry, 2007; Pesarin and Salmaso, 2010; Brombin and Salmaso, 2013; Good, 2013) is an exact non-parametric approach to statistic hypothesis testing where the data is permuted in order to capture the behaviour of a test statistic under the null hypothesis. The biggest impediment to its universal use is the computational burden of simulating massive numbers of permutations of one’s dataset. To solve this problem, the recent work of Kashlak et al. (2020) proposes an analytic approach to computing p-values from permutation tests for two-sample and k -sample testing for complex data types like speech sounds. Such analytic permutation testing was extended to LISA and GISA statistics for univariate spatial data in Kashlak and Yuan (2020). In this work, the previously investigated permutation testing framework is extended to spatial-temporal data specifically for the spatial panel model.

2 US County-wise Elections Data

County-wise results for US presidential elections are available online via the MIT Election Data and Science Lab (Data and Lab, 2018). We will consider the electoral results over the five

Table 1: Results of a post-hoc Tukey test comparing election years with bolded entries having significant p-values with a test size of 5%. The values in the table are column-year minus row-year.

	Year			
	2004	2008	2012	2016
2000	3.29%	-0.10%	2.67%	6.35%
2004		-3.40%	-0.62%	3.06%
2008			2.78%	6.46%
2012				3.68%

presidential elections from 2000 to 2016 inclusive. For this analysis, the states of Alaska and Hawaii were removed so that the counties considered form a connected graph. Also, three island counties were removed similarly as they have no edges in the graph; these are Dukes and Nantucket county in Massachusetts and San Juan county in Washington. Lastly Broomfield county, Colorado, was removed from the dataset as it was incorporated in 2001 and thus was not present for the election of 2000.

The observations considered are the vectors $y_i \in [0, 1]^5$ where y_{ti} is the fraction of the vote that went to the Republican candidate; George W Bush; John McCain; Mitt Romney; and Donald Trump. The predictor variables considered are the voter population density (log-scale), the state where the county resides (categorical), median income (log-scale) downloaded from the Bureau of Labor Statistics, Local Area Unemployment Statistics, and the percentage of the population that identifies as non-Hispanic white according to the U.S. Census Bureau’s Population Division. The relation between voting behaviour and each of the three continuous predictor variables is complex. Hence, we consider linear, quadratic, and cubic polynomials for each of these. Plots of these polynomials and the data are displayed in Figure 1. Comparing log voter density to Republican vote, there is a noticeable negative trend indicating that the most densely populated counties vote more heavily for the Democratic candidate. This coincides with the common assumption that dense cities tend to vote left while sparse rural areas tend to vote right. There is no strong positive or negative correlation between median income and voter behaviour, but the cubic regression nevertheless identifies a drop in the Republican vote for the poorest counties. Lastly, a quadratic polynomial shows that the Republican vote begins to drop on average as the non-Hispanic white percentage of the population drops below 60%.

For categorical predictors, boxplots of the five election years are displayed in Figure 2 and Table 1 displays the results of a post-hoc Tukey test. The boxplots and table indicate that there is no significant difference in the average countywise Republican vote between years 2000 & 2008 and 2004 & 2012. The average countywise vote was higher in 2016 for Donald Trump than in the previous years. However, Trump still received a smaller percentage of the popular vote than Hillary Clinton, the Democratic challenger. Due to the subtleties of the electoral college system used to elect a US president, a candidate’s county-wise performance does not completely dictate the outcome of the election. Aggregated over the five years of elections, the median countywise Republican vote was 60.1% with 1st and 3rd quartiles of 50.5% and 69.6%. However, the overall Republican popular vote—i.e. aggregated Republican votes over all five elections divided by total votes cast—is only 47.4%. Boxplots are also plotted in Figure 3 for each US state aggregated over all counties and the five elections. These are ordered from smallest to largest median county Republican vote.

Republican Votes by Predictors

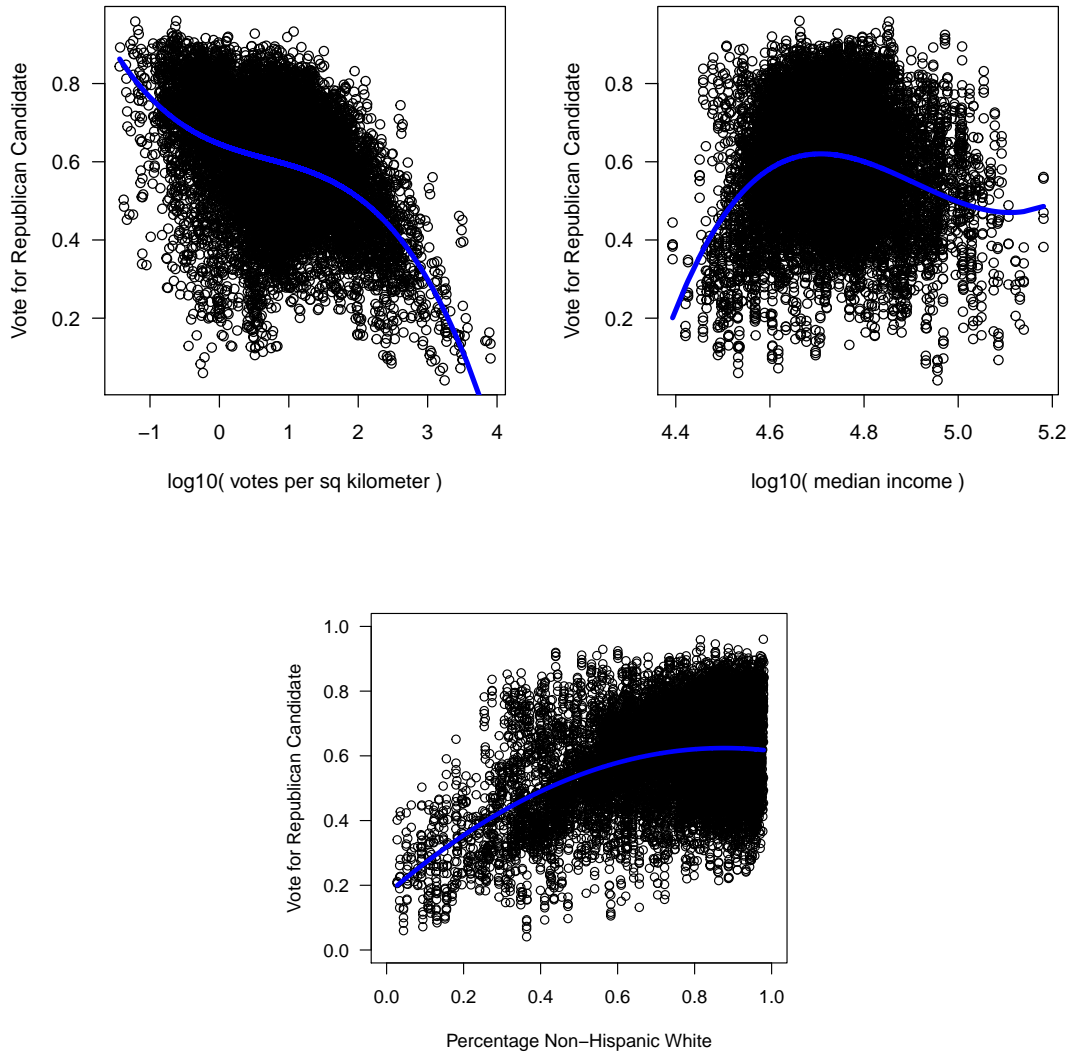


Figure 1: The fraction of the vote for the Republican candidate plotted against \log_{10} voter population density (top left, $R^2 = 0.196$), \log_{10} median income (top right, $R^2 = 0.071$), and percentage of the population that is non-Hispanic white (bottom, $R^2 = 0.143$). The blue lines are cubic polynomials fit by least squares for the top plots and a quadratic polynomial for the bottom.

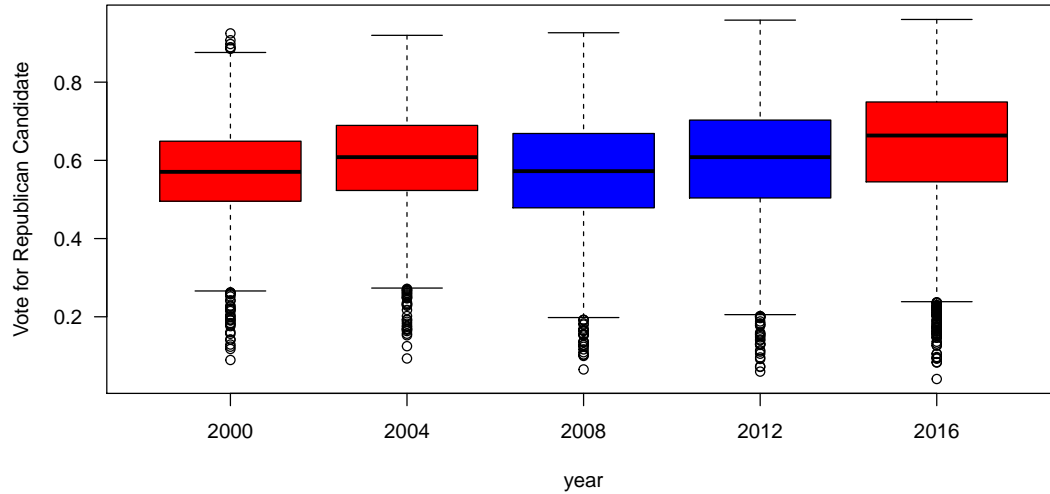


Figure 2: Boxplots of the vote percentages for each year in the dataset coloured by the winning candidate (red = Republican, blue = Democrat).

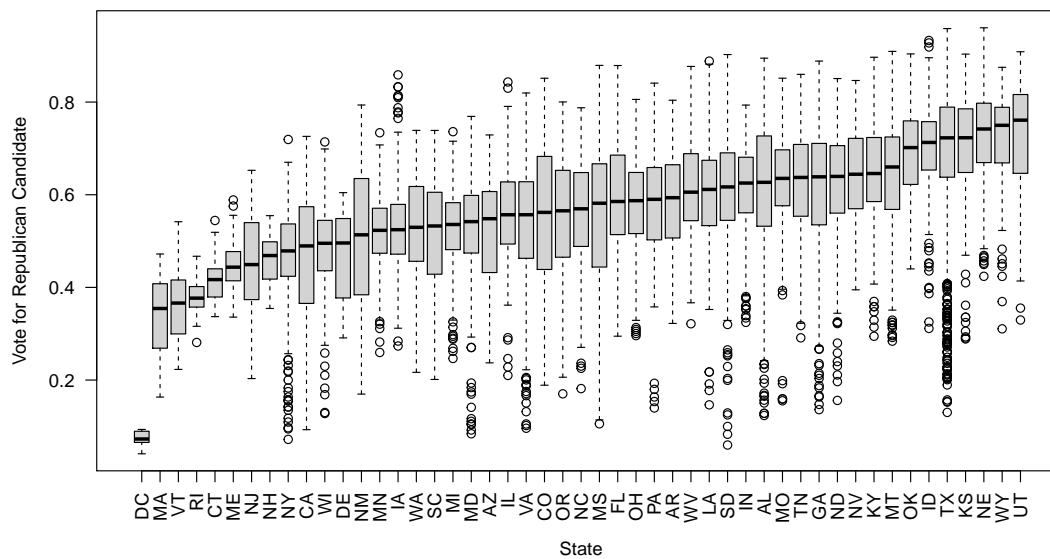


Figure 3: Boxplots of the vote percentages for each state in the dataset ordered from smallest to largest median Republican vote.

3 Local Spatial Association

3.1 LISA Statistics

Given spatial measurements or residuals from a fitted spatial model, it is desirable to identify ‘hot spots’ being any spatial region where the observations are correlated. This led to the development of many Local Indicators of Spatial Association (LISA) statistics (Cliff and Ord, 1981; Sokal et al., 1998; Waller and Gotway, 2004; Getis and Ord, 2010; Gaetan and Guyon, 2010; Luo et al., 2019; Seya, 2020). In what follows, we ignore normalizing constants as our entire approach centers around permutation testing which is invariant to such constants.

For univariate data, we can define a few different LISA statistics. Let \mathcal{G} be a graph with n vertices ν_1, \dots, ν_n and real valued measurements $y_1, \dots, y_n \in \mathbb{R}$ at each vertex. For any choice of $n \times n$ weight matrix W , Local Moran’s index for vertex i is

$$I_i \sim \sum_{j=1}^n w_{i,j} (y_i - \bar{y})(y_j - \bar{y})$$

where $w_{i,j}$ is the i, j th entry of W . Local Geary’s statistic for vertex i is defined as

$$C_i \sim \sum_{j=1}^n w_{i,j} (y_i - y_j)^2.$$

The rank correlation statistic presented in Kashlak and Yuan (2020) and referred to as binary association is

$$B_i \sim \beta_i \sum_{j=1}^n w_{i,j} \beta_j, \quad \beta_i = \begin{cases} 1, & y_i \geq m \\ -1, & y_i < m \end{cases}$$

for $m = \text{median}(y)$. The classic Gettis-Ord statistics are not included here as they are equivalent to Moran’s index under the permutation methodology.

For multivariate data, let $y_i \in \mathbb{R}^T$ be a T -long vector for the i th vertex. These univariate LISA statistics can be extended to this setting as follows. For a fixed symmetric positive definite $T \times T$ matrix M , an inner product on \mathbb{R}^T can be defined as $\langle a, b \rangle_M = a^T M b$ for any $a, b \in \mathbb{R}^T$. Thus, for any such choice of M , the vector version of Moran’s statistic is

$$I_i \sim \sum_{j=1}^n w_{i,j} \langle y_i - \bar{y}, y_j - \bar{y} \rangle_M$$

where we again ignore scaling constants. For $Y = (y_1 \ y_2 \ \dots \ y_n) \in \mathbb{R}^{T \times n}$, this statistic can be quickly computed at every vertex via the formula

$$I = \text{diag} \left[(Y - \bar{Y})^T M (Y - \bar{Y}) W \right] \in \mathbb{R}^n$$

where $\text{diag}[A]$ extracts the diagonal of matrix A and $\bar{Y} = (\bar{y} \ \bar{y} \ \dots \ \bar{y})$. Geary’s statistic can be extended to multivariate data by simply considering

$$C_i \sim \sum_{j=1}^n w_{i,j} \|y_i - y_j\|_{\ell^p}^p$$

for some choice of ℓ^p norm. For the Euclidean norm, this can be computed for all vertices quickly as $\|y_i - y_j\|_{\ell^2}^2 = \|y_i\|_{\ell^2}^2 + \|y_j\|_{\ell^2}^2 - 2 \langle y_i, y_j \rangle$. Noting that the matrix $Y^T Y$ has i, j th entry $\langle y_i, y_j \rangle$ and setting $d = \text{diag}(Y^T Y)$,

$$C = \text{diag} \{ [(d \oplus d) - 2Y^T Y] W \} \in \mathbb{R}^n$$

Table 2: Choices of matrices A and B to get a γ_i equivalent to one of the LISA statistics.

LISA	$A_{i,j}$	$B_{i,j}$
Moran	$w_{i,j}$	$\langle y_i - \bar{y}, y_j - \bar{y} \rangle_M$
Geary	$w_{i,j}$	$\ y_i - y_j\ _{\ell^p}^p$
Binary	$w_{i,j}$	$\langle \beta_i, \beta_j \rangle$

where $(d \oplus d)_{i,j} = d_i + d_j$. Lastly, the binary association statistic can be simply generalized to the multivariate setting in the same manor as with Moran's index:

$$B_i \sim \sum_{j=1}^n w_{i,j} \langle \beta_i, \beta_j \rangle, \quad \beta_{i,k} = \begin{cases} 1, & y_{i,k} \geq m_k \\ -1, & y_{i,k} < m_k \end{cases}$$

for $m_k = \text{median}(y_{i,k} : i = 1, \dots, n)$. For binary association, we just consider the standard Euclidean inner product, i.e. the dot product.

3.2 Significance Testing

3.2.1 Local Testing

A general approach to testing LISA statistics by analytically bounding the permutation test p-value is introduced in [Kashlak and Yuan \(2020\)](#). Here, we extend this work to the multivariate setting.

The gamma index ([Mantel, 1967](#); [Hubert, 1985](#)) is a general measure of matrix similarity, $\gamma_{AB} := \sum_{i,j=1}^n a_{i,j} b_{i,j}$, for two similar matrices A and B . For specific choices of A and B , the gamma index can be treated as a general correlation statistic. The local gamma index ([Anselin, 1995](#)) is similarly defined as $\gamma_i = \sum_{j=1}^n a_{i,j} b_{i,j}$. The formulae from Section 3.1 can be rewritten in terms of a local gamma index by choosing A to be the weight matrix W and B to be one of the entries in Table 2. To align with the notation of [Anselin \(1995\)](#) and [Kashlak and Yuan \(2020\)](#), we will write $a_{i,j} = w_{i,j}$, $b_{i,j} = \lambda(y_i, y_j)$ for some similarity function λ , and finally that $\gamma_i = \sum_{j=1}^n w_{i,j} \lambda(y_i, y_j)$. Using this notation, we can define the permuted local gamma index to be $\gamma_i(\pi) = \sum_{j=1}^n w_{i,j} \lambda(y_i, y_{\pi(j)})$ where π is a uniformly random element of \mathbb{S}_n , the symmetric group on n elements, conditioned so that $\pi(i) = i$.

In [Kashlak and Yuan \(2020\)](#), it is proven that for any such gamma index constructed with a binary weight matrix—i.e. $w_{i,j} = 0, 1$ for all $i, j = 1, \dots, n$ —the following concentration inequality holds when $m_i = \sum_{j=1}^n w_{i,j} \ll n/2$ or $m_i \gg n/2$,

$$\mathbb{P}(|\gamma_i(\pi) - m_i \bar{\lambda}_{-i}| \geq \gamma_i \mid y_1, \dots, y_n) \leq \frac{1}{\sqrt{\pi}} \Gamma\left(\frac{n-1}{m_i(n-m_i-1)} \frac{\gamma_i^2}{2s_i^2}; \frac{1}{2}\right) + O(n^{-4}) \quad (3.1)$$

where $\mathbb{P}(\cdot)$ is the uniform probability measure on the symmetric group conditioned so that $\pi(i) = i$, $\bar{\lambda}_{-i} = (n-1)^{-1} \sum_{j=1}^n \lambda(y_i, y_j) \mathbf{1}_{i \neq j}$, $\Gamma(\cdot)$ is the upper incomplete gamma function, and $s_i^2 = (n-1)^{-1} \sum_{j \neq i} (\lambda_{i,j} - \bar{\lambda}_{-i})^2$ is the sample variance of the i th row.

Remark 3.1. Typically, for planar data such as that considered in this work, $m_i \ll n/2$ for all vertices $i = 1, \dots, n$. However, in the case where $m_i \sim n/2$, we define

$$\begin{aligned} \omega_- &= \min\{m_i, n - m_i - 1\} / \max\{m_i, n - m_i - 1\}^2, \text{ and} \\ \omega_+ &= \max\{m_i, n - m_i - 1\} / \min\{m_i, n - m_i - 1\}^2. \end{aligned}$$

Then, the concentration inequality becomes

$$P(|\gamma_i(\pi) - m_i \bar{\lambda}_{-i}| \geq \gamma_i \mid y_1, \dots, y_n) \leq C_0 I \left[\exp \left(-\frac{\gamma_i^2}{2s_i^2} \varpi_- \right); (n-1)\varpi_+, \frac{1}{2} \right]$$

where $I[\cdot]$ is the regularized incomplete beta function, and $C_0 = \frac{\sqrt{(n-1)\varpi_+} \Gamma((n-1)\varpi_+)}{\Gamma(\frac{1}{2} + (n-1)\varpi_+)}$ with $\Gamma(\cdot)$ the (complete) gamma function.

3.2.2 Global Testing

Statistics for local indicators of spatial association can be extended to statistics for global indicators of spatial association (GISA). In [Kashlak and Yuan \(2020\)](#), a concentration inequality similar to that for LISA statistics is proved. Given the same setup as the previous section, then

$$P \left(\left| \gamma(\boldsymbol{\pi}) - \sum_{i=1}^n m_i \bar{\lambda}_{-i} \right| \geq \gamma \mid y_1, \dots, y_n \right) \leq \frac{1}{\sqrt{\pi}} \Gamma \left(\frac{\gamma^2}{4v^2}; \frac{1}{2} \right) + O(2^{-2n}) \quad (3.2)$$

where $\boldsymbol{\pi} = (\pi_1, \dots, \pi_n)$ with $\pi_i(i) = i$, $\gamma(\boldsymbol{\pi}) = \sum_{i=1}^n \gamma_i(\pi_i)$ is the permuted variant of this test statistic, and $v^2 = \sum_{i=1}^n \eta_i s_i^2$ with $\eta_i = m_i(n - m_i - 1)/(n - 1)$.

The GISA tests apply to the same statistics as the LISA tests do. These GISA test statistics are more directly comparable with the LM and LR tests considered in [Breusch and Pagan \(1980\)](#); [Anselin and Bera \(1998\)](#); [Baltagi et al. \(2003\)](#); [Hsiao \(2014\)](#) and others.

4 Simulation Studies

4.1 LISA Tests

Four LISA statistics—Moran, Geary ℓ^2 and ℓ^1 , and Binary association—are tested on simulated data on a (50×60) -vertex rectangular grid where up to four edges exist for each vertex connecting it to those vertices above and below and to the left and to the right. Denoting the graph adjacency matrix as A , we generate 200 replicates of mean zero 5×3000 dimensional multivariate Gaussian data with covariance $I + cA$ where $c \in [-0.25, 0.25]$.

Figure 4 charts the number of vertices with p-values less than 5% for each of the four LISA statistics with p-values computed via formula 3.1. As c increases from zero, Moran’s statistic is shown to identify the most significant vertices followed by Geary with the ℓ^1 norm. Geary ℓ^2 and binary association perform the worst. In contrast, for c decreasing invoking negative correlations between adjacent vertices, the power curves for Moran and Geary ℓ^2 show similar performance with Geary ℓ^1 identifying fewer significant vertices and with binary association performing the worst.

In these simulations, the binary association statistic performed the worst in both testing scenarios. However, in the next section, it is shown to have good performance on the US elections data while Geary with the ℓ^2 norm identified the fewest hot spots. Moran’s statistic consistently achieves the highest power in all testing scenarios. However, the other three methods often identify vertices missed by Moran’s statistic. This suggests that these LISA statistics can be used to complement one another in an exploratory analysis.

4.2 GISA Tests

Testing for global spatial association (GISA) is also possible using formula 3.2. Computing p-values for the same simulated data and test statistics considered above results in Figure 5.

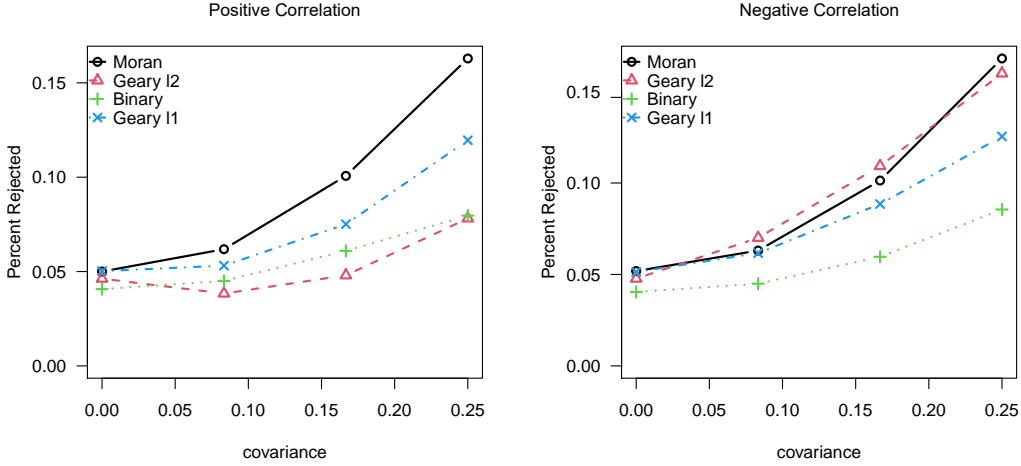


Figure 4: Power curves for the four LISA tests as the covariance increases in the positive direction (left) and negative direction (right).

For positively correlated neighbours, the global version of Moran’s test gives the best statistical power. Geary’s ℓ^2 and then ℓ^1 statistics are next, and the global binary association test performs the worst, but still is able to achieve a good amount of power to identify the presence of global spatial association. Similar behaviour is seen for a negatively correlated network. Of note, Geary’s ℓ^2 global test gives slightly higher power than Geary’s ℓ^1 whereas for local testing, Geary with the ℓ^1 norm has stronger performance than ℓ^2 for positively correlated data.

In the real data sections to follow, we do not discuss GISA testing as all of the p-values are extremely small for all four statistics and all five neighbourhoods considered. This is evident in the LISA plots displayed below in Figure 7, which show many areas of spatial association under each of the four statistics considered.

5 Real Data Results

5.1 Spatial Panel Data Regression

Fitting and testing a spatial panel model requires selection of a weight matrix. To coincide with the theorems in [Kashlak and Yuan \(2020\)](#), we will only consider binary weight matrices—i.e. those with entries 0 and 1 only. Among such weight matrices, we denote W_k to be the k -lagged weight matrix. Beginning with $W_0 = I$ and W_1 being the graph adjacency matrix, we recursively define

$$W_k = W_1^k \prod_{l=0}^{k-1} (\mathbf{1} - W_l)$$

where $\mathbf{1}$ is the $n \times n$ matrix of all ones. We will consider neighbourhoods for $k = 1, \dots, 5$.

The fitted spatial panel models are compared in Table 3. Both λ , the spatial lag parameter, and ρ , the spatial autocorrelated errors parameter, decrease in magnitude as the lag increases. Thus, the spatial dependence in the data begins to wane as the neighbourhood spreads out.

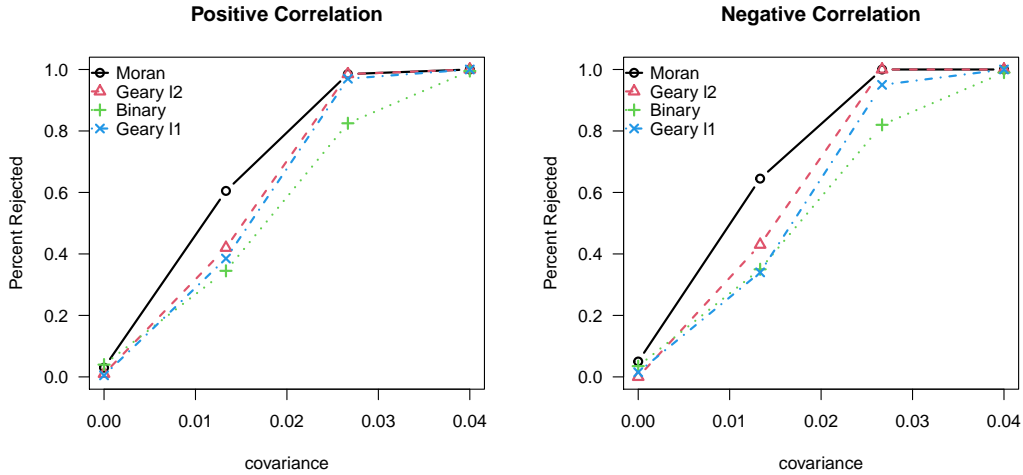


Figure 5: Power curves for the four GISA tests as the covariance increases in the positive direction (left) and negative direction (right).

Table 3: A comparison of spatial panel models for neighbourhoods defined by lags 1, . . . , 5.

	Lag				
	1	2	3	4	5
λ	0.0225	0.0094	0.0035	0.0018	0.0013
ρ	-0.0779	-0.0180	0.0051	0.0086	0.0088
σ_v^2	0.0024	0.0023	0.0024	0.0023	0.0023
σ_μ^2	0.0242	0.0238	0.0238	0.0238	0.0239
R^2	59.4%	62.2%	62.9%	63.1%	63.1%

Thus, in the next section, we will focus on testing for local spatial association with the adjacency weight matrix. The R^2 values for the five fitted models all are around 60%.

Fitting a spatial panel data regression model to this data captures the behaviour of voting in most US counties. However, extreme counties with respect to the predictors result in inaccurate or erroneous predictions. On the political left, the counties of New York City and the Bronx both have fitted values less than zero. NYC has the highest voter density with between 7000 and 8000 voters per square kilometre across the five elections. The next densest county is King’s County, NY with approximately 3500 voters per square kilometer. The Bronx is also one of the counties with the densest population, but while NYC is about 47% white and King’s is 37.5% white, the Bronx is less than 10% white. On the political right, both King and Loving county, Texas, get fitted values greater than 100%. This is mainly due to being very sparsely populated (~ 1 voter per 20 square kilometers) and in Texas, which gives a boost to the expected Republican vote as discussed next.

Inclusion of the state as a categorical predictor allows us to identify those states that vote more or less favourably for the Republican candidate than the three continuous predictors—population density, median income, and non-Hispanic whiteness—would suggest. Most notably, the state of Texas has an estimated upward shift of 19.2% indicating that Texan counties on average vote more heavily for the Republican candidate than expected given the other predictors.

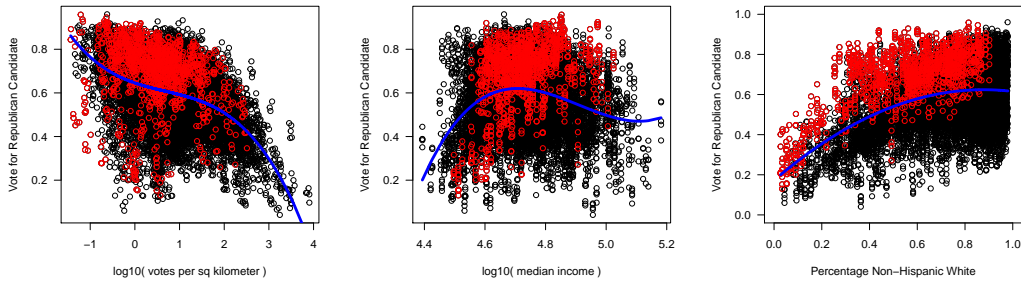


Figure 6: A copy of Figure 1 with the Texas counties coloured in red. This demonstrates a higher percentage of Texan vote going towards the Republican candidate than expected by the three predictors.

This is visualized in Figure 6, which shows the fitted regression lines for the three predictors with Texan counties coloured in red. The majority of Texan counties lie above the regression lines.

5.2 Local Spatial Association

Four multivariate LISA statistics are applied to the residuals for the fitted models. These are Moran’s I , Geary’s statistic in both ℓ^2 and ℓ^1 , and binary association. The p-values produced by formula 3.1 are subsequently adjusted for multiple testing using the Benjamini-Hochberg method for False Discovery Rate (FDR) control within the spatial framework making use of the `p.adjustSP` function in the `spdep` R package (Bivand and Wong, 2018; Bivand et al., 2013). The p-values reported were computed with W_1 , the adjacency matrix, as the chosen weight matrix. Similar results were seen for other weight matrices.

Counties with significant p-values under each of the LISA statistics are displayed in Figure 7, which are coloured by red or blue depending on whether the Republican or Democratic candidate took more than 50% of the county’s vote in three or more of the years considered. This allows for the visualization of hot spots where the residuals all trend in a similar direction. Moran’s statistic finds the most significant counties of the four methods; 18.5% of the 3104 counties are designated as significant at an FDR of 5%. Binary association comes next at 13.6%, Geary’s statistic with the ℓ^1 norm at 9.4% and lastly Geary’s statistic with ℓ^2 with only 2.6% of the counties deemed to have significant spatial association after correcting for multiple testing. The lighter colours indicate significant at 5% FDR and the darker colours indicate significant at 1% FDR.

LISA statistics can detect both significant positive and negative spatial association. However, nearly all of the counties detected in Figure 7 are due to positive association. As these statistics are computed on the residuals produced from the spatial panel model, positive spatial association implies the existence of a geographic region where the residuals trend in the same direction. These are geographic voting blocks whose votes trend in a similar direction even after the three predictors and US state are taken into account. One of the most noticeable correlated collections of counties is the Republican voting north-south region spanning from west Texas upward through the Kansas-Colorado border. Another Republican voting block exists around the boarder of Kentucky with Virginia and West Virginia extending into Tennessee. The Moran,

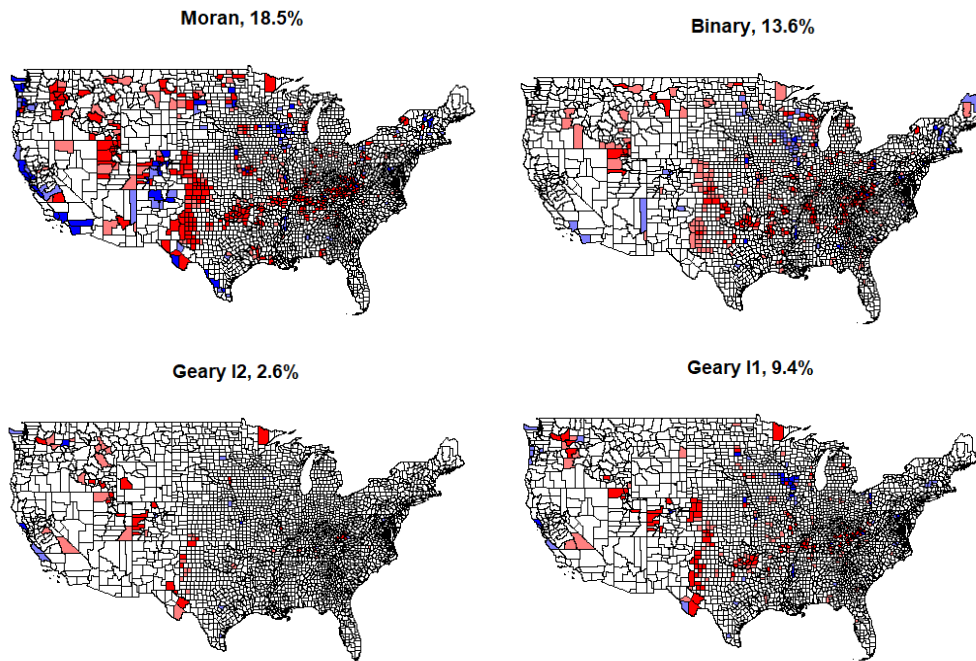


Figure 7: Maps displaying significant counties with respect to a given LISA statistic after adjusting for multiple testing. The percentage of significant counties is displayed in the plot titles.

binary, and ℓ^1 Geary maps highlight a Democrat voting region along the Mississippi river as it separates the states of Iowa and Minnesota from Illinois and Wisconsin. The Moran map also detects significant spatial autocorrelation along the left-voting west coast counties.

5.3 Comparison of LISA Statistics

In the previous section, Figure 7 shows that the number of significant counties detected can vary a lot between the four methods. To further contrast the four methods, we can consider 2×2 tables for the agreements and disagreements between each pair of methods. In Table 4, the Matthews Correlation Coefficient,

$$\text{MCC} = \frac{TP \times TN - FP \times FN}{\sqrt{(TP + FP)(TP + FN)(TN + FP)(TN + FN)}},$$

and the Rand index,

$$\text{Rand} = \frac{TP + TN}{TP + FP + FN + TN},$$

are computed for each pairing of methods. For simplicity of notation, we use true/false positive/negative to refer to the methods agreeing or disagreeing on which counties are chosen have significant spatial association.

The Rand index or percentage of agreement is above 80% for each pairing of methods. This is due to most of the counties being deemed non-significant (TN) by all methods. The MCC

Table 4: A comparison of the four LISA statistics using Matthews Correlation (left) and using the Rand Index (right).

	MCC			Geary ℓ^2	Rand	
	Geary ℓ^2	Geary ℓ^1	Binary		Geary ℓ^1	Binary
Moran	0.232	0.437	0.447	0.828	0.855	0.849
Geary ℓ^2		0.394	0.132		0.860	0.922
Geary ℓ^1			0.412			0.878

gives a more nuanced comparison of the methods. Higher MCCs are seen for Moran and Binary association, both of which are of the form of an inner product, and for Geary ℓ^1 and ℓ^2 , both of which are of the form of an ℓ^p norm.

6 Discussion and Extensions

There are many ways to test for local and global spatial association for spatial panel data models. In this work, we have seen that the extension of Moran’s statistic to the multivariate domain gives the best power to identify local clusters of spatially dependent regions. However, other methods have both comparable statistical power and typically identify different significant regions. Thus, an ensemble approach to detecting spatially dependent regions is warranted.

The extensions of LISA statistics presented in Section 3.1 are based on inner products (Moran and binary association) and on ℓ^p norms (Geary). This naturally can be further applied to spatially observed functional data such as climate data, linguistic data, and others (Delicado et al., 2010; Menafoglio and Petris, 2016; Tavakoli et al., 2019). Panel data, longitudinal data, functional data, and time series data are all closely related objects of study that often are collected from a spatial domain. Our methodology is extendable to such areas of analysis.

Acknowledgements

The authors would like to thank the Natural Sciences and Engineering Research Council of Canada (NSERC) for their funding support.

References

- Luc Anselin. Local indicators of spatial association—lisa. *Geographical analysis*, 27(2):93–115, 1995.
- Luc Anselin. A local indicator of multivariate spatial association: extending geary’s c. *Geographical Analysis*, 51(2):133–150, 2019.
- Luc Anselin and Anil K Bera. Spatial dependence in linear regression models with an introduction to spatial econometrics. *Statistics textbooks and monographs*, 155:237–290, 1998.
- Luc Anselin et al. Spatial econometrics. *A companion to theoretical econometrics*, 310330, 2001.
- Badi H Baltagi, Seuck Heun Song, and Won Koh. Testing panel data regression models with spatial error correlation. *Journal of econometrics*, 117(1):123–150, 2003.
- Badi Hani Baltagi. *Econometric analysis of panel data*, volume 4. Springer, 2008.

- Roger Bivand and David W. S. Wong. Comparing implementations of global and local indicators of spatial association. *TEST*, 27(3):716–748, 2018. URL <https://doi.org/10.1007/s11749-018-0599-x>.
- Roger S. Bivand, Edzer Pebesma, and Virgilio Gomez-Rubio. *Applied spatial data analysis with R, Second edition*. Springer, NY, 2013. URL <http://www.asdar-book.org/>.
- Trevor S Breusch and Adrian R Pagan. The lagrange multiplier test and its applications to model specification in econometrics. *The review of economic studies*, 47(1):239–253, 1980.
- Chiara Brombin and Luigi Salmaso. *Permutation tests in shape analysis*, volume 15. Springer, 2013.
- Andrew David Cliff and J Keith Ord. *Spatial processes: models & applications*. Taylor & Francis, 1981.
- MIT Election Data and Science Lab. County Presidential Election Returns 2000-2020, 2018. URL <https://doi.org/10.7910/DVN/VOQCHQ>.
- Pedro Delicado, Ramón Giraldo, Carlos Comas, and Jorge Mateu. Statistics for spatial functional data: some recent contributions. *Environmetrics: The official journal of the International Environmetrics Society*, 21(3-4):224–239, 2010.
- Carlo Gaetan and Xavier Guyon. *Spatial statistics and modeling*, volume 90. Springer, 2010.
- Arthur Getis and J Keith Ord. The analysis of spatial association by use of distance statistics. In *Perspectives on spatial data analysis*, pages 127–145. Springer, 2010.
- Phillip Good. *Permutation tests: a practical guide to resampling methods for testing hypotheses*. Springer Science & Business Media, 2013.
- Cheng Hsiao. *Analysis of panel data*. Number 54. Cambridge university press, 2014.
- Lawrence J Hubert. Combinatorial data analysis: association and partial association. *Psychometrika*, 50(4):449–467, 1985.
- Mudit Kapoor, Harry H Kelejian, and Ingmar R Prucha. Panel data models with spatially correlated error components. *Journal of econometrics*, 140(1):97–130, 2007.
- Adam B Kashlak and Weicong Yuan. Computation-free nonparametric testing for local and global spatial autocorrelation with application to the canadian electorate. *arXiv preprint arXiv:2012.08647*, 2020.
- Adam B Kashlak, Sergii Myroshnychenko, and Susanna Spektor. Analytic permutation testing via Kahane–Khintchine inequalities. *arXiv preprint arXiv:2001.01130*, 2020.
- Qing Luo, Daniel A Griffith, and Huayi Wu. Spatial autocorrelation for massive spatial data: verification of efficiency and statistical power asymptotics. *Journal of Geographical Systems*, 21(2):237–269, 2019.
- Nathan Mantel. The detection of disease clustering and a generalized regression approach. *Cancer research*, 27(2 Part 1):209–220, 1967.
- Alessandra Menafoglio and Giovanni Petris. Kriging for hilbert-space valued random fields: The operatorial point of view. *Journal of Multivariate Analysis*, 146:84–94, 2016.

- Paul W Mielke and Kenneth J Berry. *Permutation methods: a distance function approach*. Springer Science & Business Media, 2007.
- Giovanni Millo and Gianfranco Piras. splm: Spatial panel data models in R. *Journal of Statistical Software*, 47(1):1–38, 2012. URL <http://www.jstatsoft.org/v47/i01/>.
- Fortunato Pesarin and Luigi Salmaso. *Permutation tests for complex data: theory, applications and software*. John Wiley & Sons, 2010.
- Hajime Seya. Global and local indicators of spatial associations. In *Spatial Analysis Using Big Data*, pages 33–56. Elsevier, 2020.
- Robert R Sokal, Neal L Oden, and Barbara A Thomson. Local spatial autocorrelation in a biological model. *Geographical Analysis*, 30(4):331–354, 1998.
- Shahin Tavakoli, Davide Pigoli, John AD Aston, and John S Coleman. A spatial modeling approach for linguistic object data: Analyzing dialect sound variations across great britain. *Journal of the American Statistical Association*, 114(527):1081–1096, 2019.
- Lance A Waller and Carol A Gotway. *Applied spatial statistics for public health data*, volume 368. John Wiley & Sons, 2004.